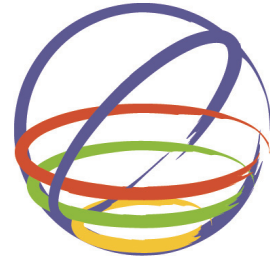


# **Effect of Strong Vertical Excitation on the Seismic Performance of RC Bridge Columns**



**H. Matsuzaki**  
*Tohoku University, Japan*

**Y. Kumagai & K. Kawashima**  
*Tokyo Institute of Technology, Japan*

**15 WCEE**  
LISBOA 2012

## **SUMMARY:**

This paper presents the effects of varying axial force including tension developed by near-field extreme vertical ground motions on the seismic performance of RC bridge columns investigated based on cyclic loading experiments. It was shown from the experiments that the damage of core concrete progressed extensively due to the reversed cyclic axial force variation from compression to tension after the longitudinal bars buckled, which resulted in the shear deformation in the plastic hinge region. The damaged area of core concrete and the increase in the amplitude of the vertical displacement after the buckling of longitudinal bars due to the axial force variation became larger as the peak tensile force in the axial force variation increased. Restoring force under tensile axial force decreased, which caused a decrease in the accumulated dissipated energy of the RC column.

*Keywords:* *Vertical ground motion, RC bridge column, Varying axial force, Cyclic loading experiment*

## **1. INTRODUCTION**

As the intensity of ground accelerations was generally smaller in the vertical component than the lateral components, and the seismic responses of ordinary bridges are predominant in the lateral direction, the effects of the vertical component have often been disregarded in the seismic design of bridges. However, extremely high amplitude ground acceleration in the vertical component was recorded at Arleta during the 1994 Northridge, USA earthquake and Ichinoseki-nishi during the 2008 Iwate-Miyagi, Japan earthquake. The PGA of vertical ground motion at Ichinoseki-nishi reached nearly 4 times the gravity acceleration. PGA does not directly control the seismic response of a bridge, but high PGA and high frequency vertical ground motion develops a large variation from compression to tension in the axial force in a column, because the axial rigidity of a column is high in the vertical direction. If the tension induced in a reinforced concrete bridge column by a vertical excitation is large enough to develop cracks inside the column, it must affect the seismic performance of the column.

The effects of vertical ground motion on the seismic performance of RC bridges have been investigated by several researchers. Papazoglou and Elnashai (1996) showed based on analysis that strong vertical ground motion can induce significant fluctuations in the axial forces, which results in a reduction in the shear capacity and the moment capacity of the column. Button et al. (2002) recommended a re-examination of existing seismic design guidelines based on the results of linear dynamic analyses using several ground motions and structural characteristics. Kunnath et al. (2008) assessed the adequacy of requirements in SDC-2006 using several bridge configurations. Sakai and Kawashima (2002) clarified the effects of varying axial force including tension on the seismic performance of a bridge column in a moment resisting frame structure based on a cyclic loading experiment. Kim et al. (2011) investigated the response of RC bridge columns subjected to the vertical ground motion based on a hybrid loading experiment. However, it is of great interest to clarify the effects of varying axial force including tension developed by high amplitude and high frequency vertical ground accelerations such as Ichinoseki-nishi record on the seismic performance of RC bridge columns.

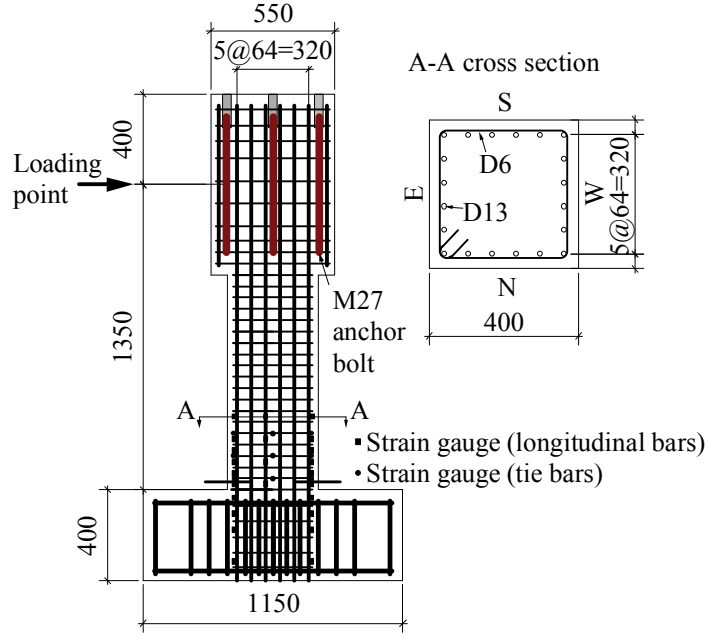


**Figure 1.** Model column

In this study, the effects of varying axial force including tension resulted from high amplitude and high frequency vertical ground acceleration on the seismic performance of RC bridge columns were investigated based on cyclic loading experiments.

## 2. EXPERIMENTAL MODELS AND LOADING PROCEDURE

### 2.1. Experimental Models

Two reinforced concrete specimens with the same section and material properties as shown in **Figure 1** were fabricated. The columns were designed in accordance with the Japanese 2002 Design Specifications of Highway Bridges (JRA, 2002). Axial stress at the plastic hinge region of the column resulted from the dead weight of a superstructure was assumed to be  $1 \text{ N/mm}^2$ . The models had a  $400 \text{ mm} \times 400 \text{ mm}$  square section, and the total height and effective height of  $1,750 \text{ mm}$  and  $1,350 \text{ mm}$ , respectively, in which the effective height represents the distance from the column base to the loading point. They were supported by  $400 \text{ mm}$  thick footings, and rigidly anchored to the loading floor by PC rods. To impose varying axial force including tensile force to the model columns, the swivel head of the vertical actuator was fixed at the column top using eight M27 anchor bolts as shown in **Figure 1**.

Twenty 13 mm diameter deformed bars with a nominal strength of  $295 \text{ N/mm}^2$  were provided for longitudinal reinforcements, and 6 mm diameter deformed bars were provided at every 50 mm interval for ties. The tie bars were anchored using 135 degree bent hooks with a development length of 100 mm. The longitudinal reinforcement ratio was 1.58 % and the volumetric ratio of tie reinforcement was 0.79 %. Yield strength of longitudinal bars and tie bars based on the coupon tests were  $374 \text{ N/mm}^2$  and  $375 \text{ N/mm}^2$ , respectively. Flexural capacity and shear capacity under the axial stress of  $1 \text{ N/mm}^2$  in compression was 119kN and 215kN based on JRA 2002, respectively, so that the columns failed in flexure.

### 2.2. Loadings

RC bridge columns are subjected to a combination of axial force variation developed by a vertical ground motion and lateral response displacement. The number of cycles of varying axial force per cycle of lateral cyclic loading is controlled by the combination of natural period in the lateral direction

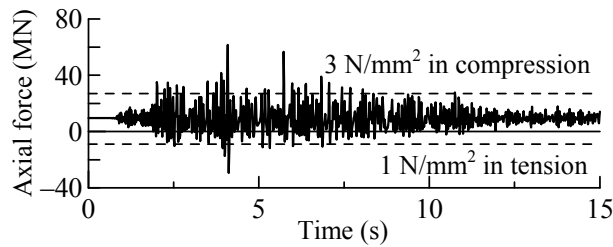


**Figure 2.** Axial force developed at the plastic hinge region of the bridge column subjected to Ichinoseki-nishi ground motion

**Table 1.** Loading conditions and material properties of model columns

Loading condition	Case 1	Case 2	Case 3	Case 4		
Number of cycles of varying axial force per cycle of lateral displacement	10	—	—	1		
Peak axial stress induced by varying axial force (N/mm <sup>2</sup> )	Tension	1.0	2.0	—		
	Compression	3.0	3.0	3.0		
Concrete compressive strength (N/mm <sup>2</sup> )	24.7		23.0			
Yield strength of longitudinal reinforcements (N/mm <sup>2</sup> )	374					
Longitudinal reinforcement ratio (%)	1.58					
Yield strength of ties (N/mm <sup>2</sup> )	375	—	363	—		
Volumetric ratio of tie reinforcement (%)	0.79					

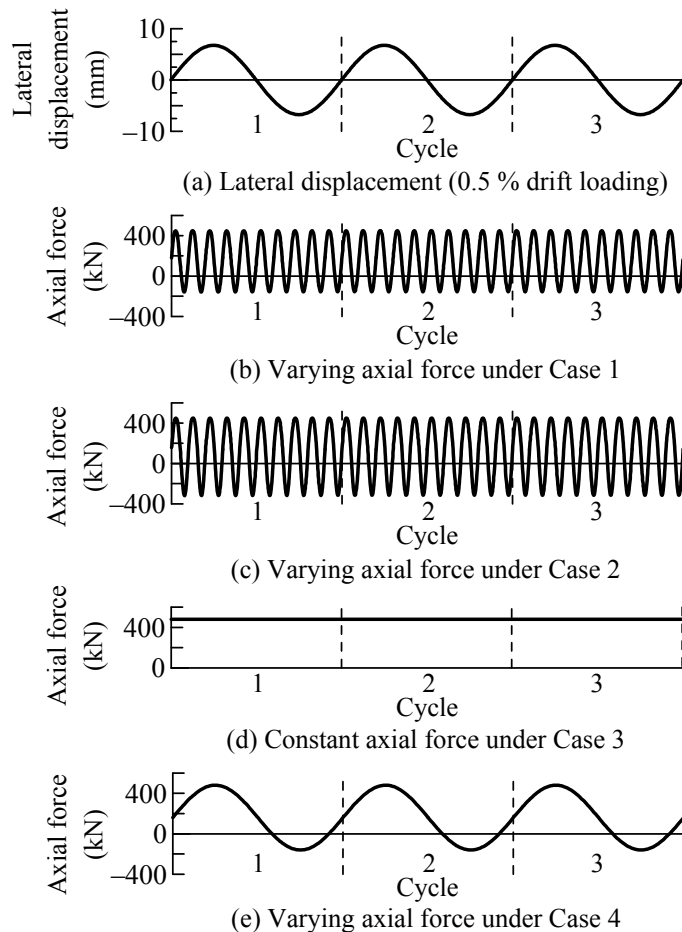


**Figure 3.** Lateral displacement and varying axial force imposed to the model column

and the vertical direction. Based on a preliminary analysis on the target column under Ichinoseki-nishi ground motion, the number of cycles of varying axial force per cycle of lateral cyclic loading was determined as 10. **Figure 2** shows the axial force developed at the plastic hinge region of the bridge

column. Varying axial force which had the peak compressive stress of  $3 \text{ N/mm}^2$  and the peak tensile stress of  $1 \text{ N/mm}^2$ , respectively, were developed continuously during the principal ground motion. Thus the peak axial stress of the varying axial force for one specimen was determined as  $1 \text{ N/mm}^2$  in tension and  $3 \text{ N/mm}^2$  in compression (denoted as Case 1 hereinafter). To investigate the effect of the peak tensile force of axial force variation on the seismic performance of RC bridge columns, varying axial force which had the peak axial stress of  $2 \text{ N/mm}^2$  in tension and  $3 \text{ N/mm}^2$  in compression was considered as another loading condition (denoted as Case 2 hereinafter).

As shown in **Table 1**, experimental results of the two columns by Sakai and Kawashima (2002) were used for comparison; one was a column subjected to a constant compressive axial stress of  $3 \text{ N/mm}^2$  (denoted as Case 3 hereinafter) and the other was a column subjected to a cycle of varying axial force which had the peak axial stress of  $1 \text{ N/mm}^2$  in tension and  $3 \text{ N/mm}^2$  in compression per cycle of lateral displacement (denoted as Case 4 hereinafter).

**Figure 3** shows the axial force and lateral displacement imposed to the columns under Case 1-4. Columns were loaded by three dynamic actuators at Tokyo Institute of Technology. In the cyclic loading, the unilateral cyclic force was imposed to the columns under the displacement control. Amplitude of the lateral displacement was increased from 0.5 % drift to failure with an increment of 0.5 % drift, in which drift is defined as the ratio of lateral displacement to the effective column height. Three cyclic loadings were imposed at each loading step.

### 3. PERFORMANCE OF COLUMNS

#### 3.1. Progress of Failure

**Figures 4** and **5** show the progress of failure under Case 1 and Case 2, respectively. Horizontal flexural cracks occurred within the region of 500 mm and 800 mm high from the column base under Case 1 and Case 2, respectively. This difference in the height of cracked region under Case 1 and Case 2 was caused because the peak tensile axial force under Case 2 was twice as large as that under Case 1. Compressive failure started to occur in the covering concrete in the plastic hinge region at 4.0 % drift

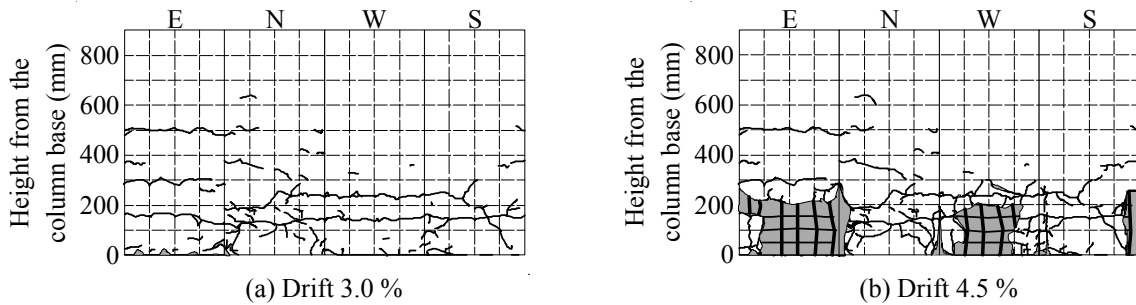


**Figure 4.** Progress of failure of column under Case 1

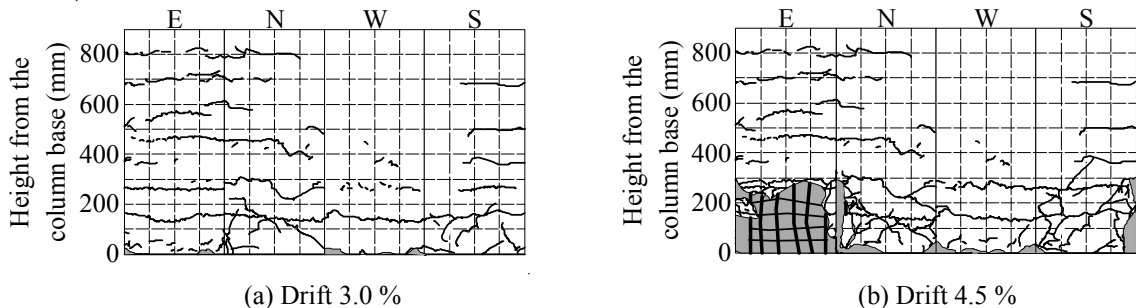


**Figure 5.** Progress of failure of column under Case 2



(a) Case 1



(b) Case 2

**Photo 1.** Damage of core concrete after 5.5 % drift loading

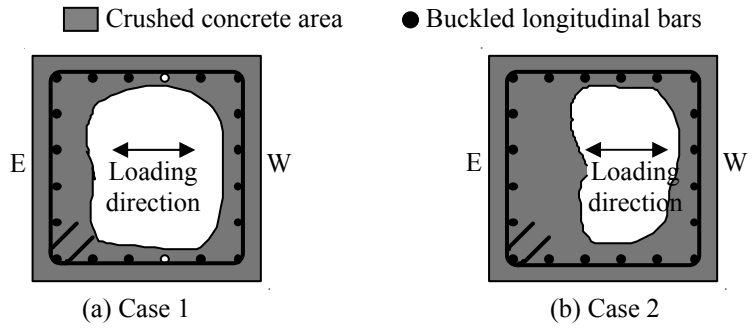


**Figure 6.** Damage of plastic hinge region after 5.5 % drift loading

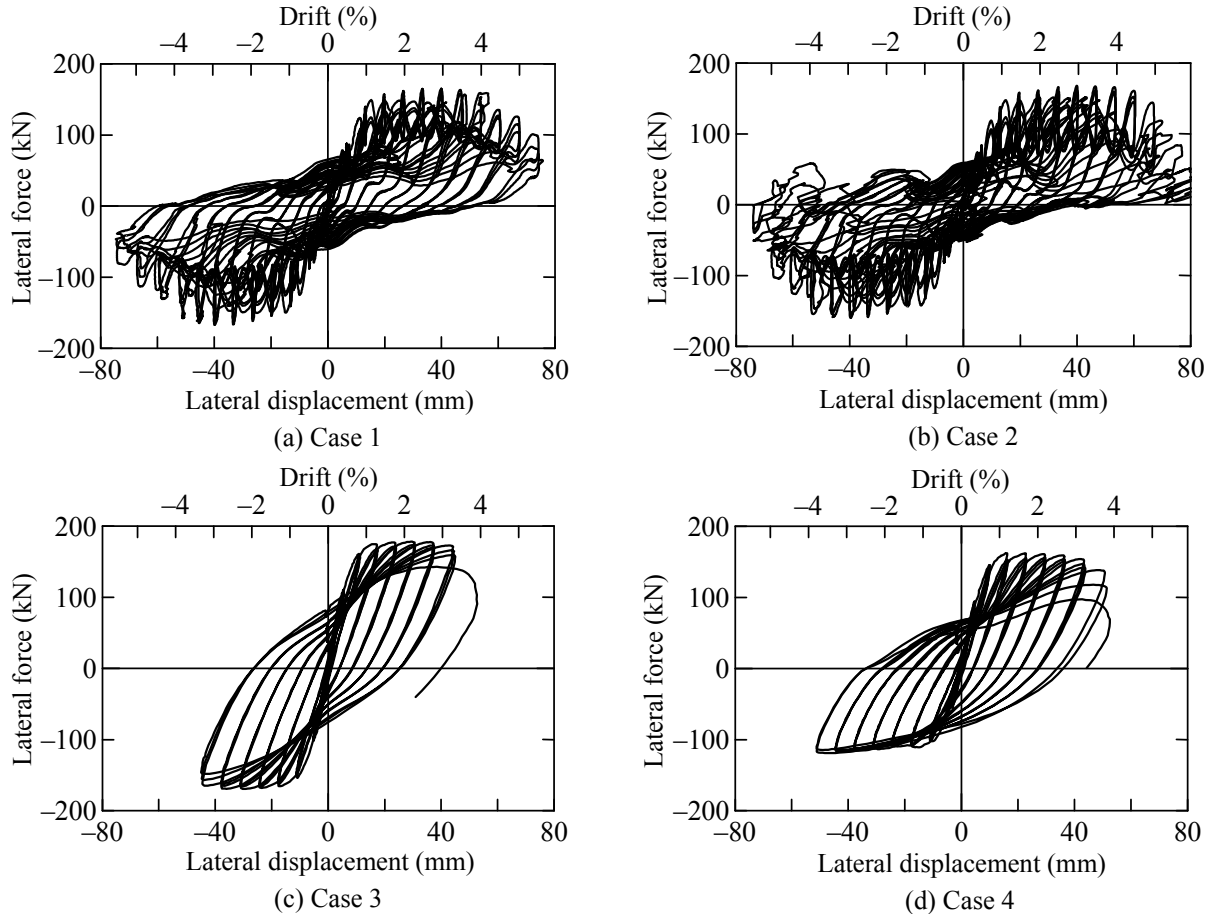


**Figure 7.** Lateral force vs. lateral displacement hysteresis

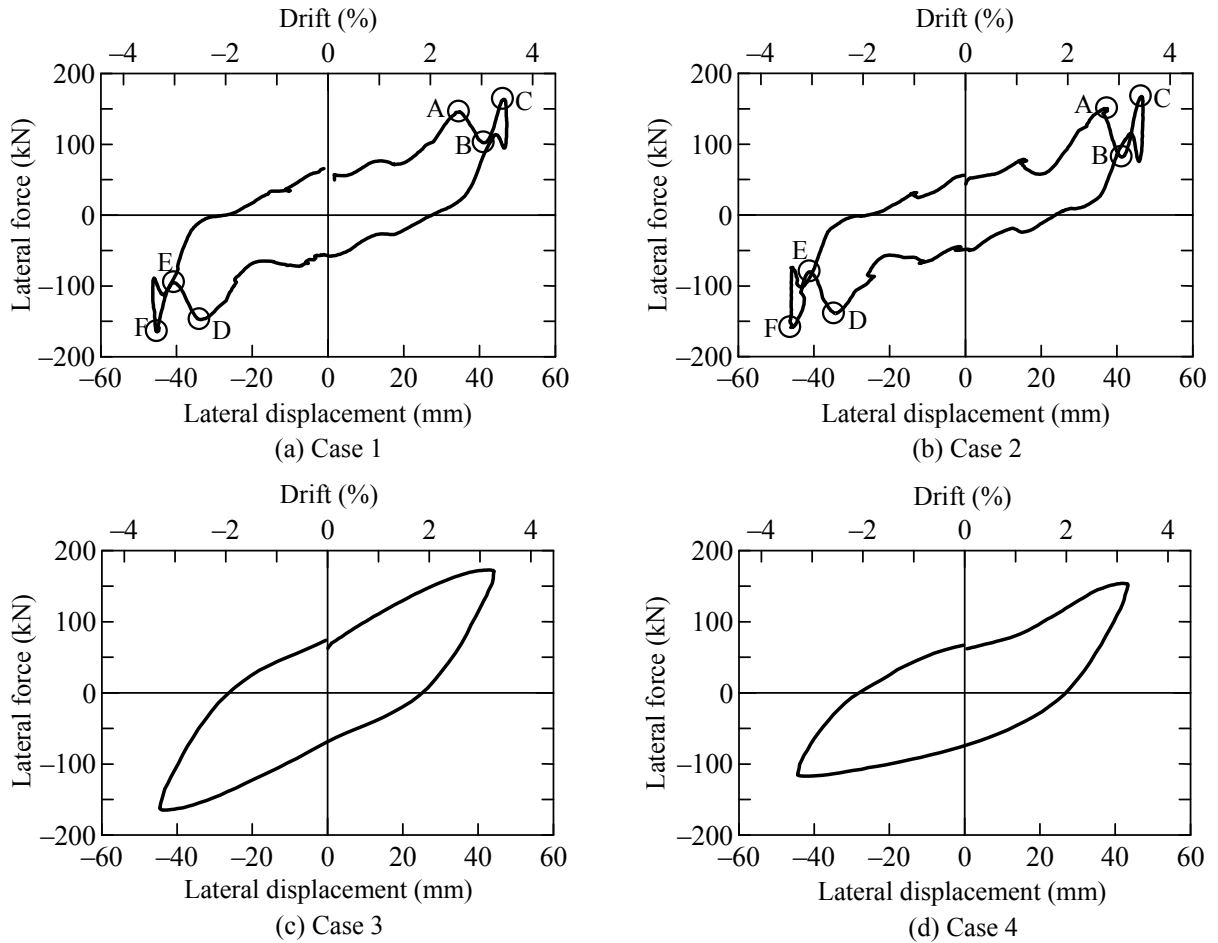


**Figure 8.** Lateral force vs. lateral displacement hysteresis at 3.5 % drift loading

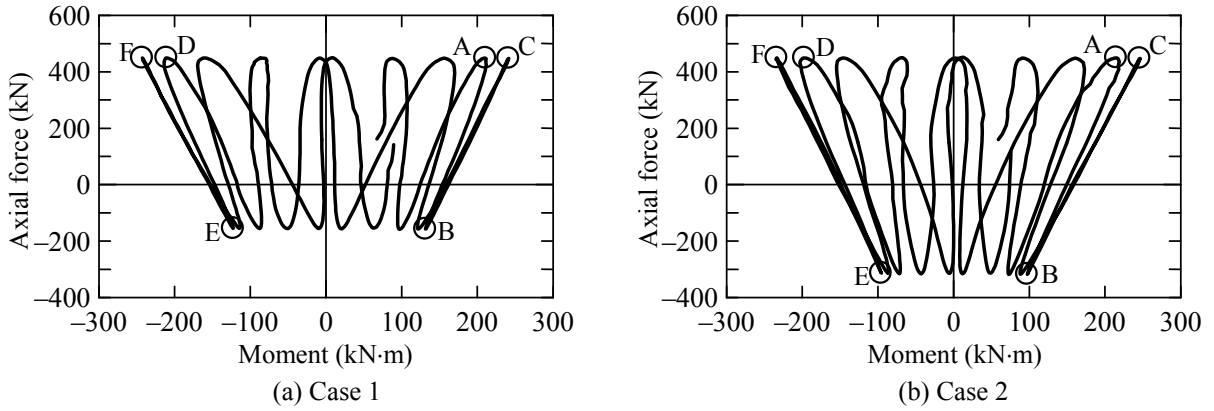


**Figure 9.** Axial force vs. moment hysteresis at 3.5 % drift loading

loading on E face. At 4.5 % drift loading, the covering concrete started to spall off, and longitudinal and tie bars were exposed. Compressive failure of core concrete at the plastic hinge region progressed severely under the reversed cyclic varying axial force after longitudinal bars buckled.

The loading was terminated after 5.5% drift loading because some longitudinal bars were ruptured and the lateral force capacity started to deteriorate under Case 1 as well as Case 2. **Photo 1** shows the damage of plastic hinge region after the removal of the covering concrete after 5.5 % drift loading. **Figure 6** shows the damage of core concrete and longitudinal bars after 5.5 % drift loading. The damage of core concrete was the most extensive at 130 mm high from the column base. Damaged area of core concrete was larger under Case 2 than Case 1 as shown in **Figure 6**.

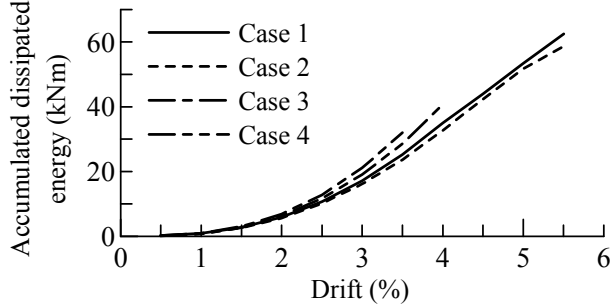


**Figure 10.** Accumulated dissipated energy

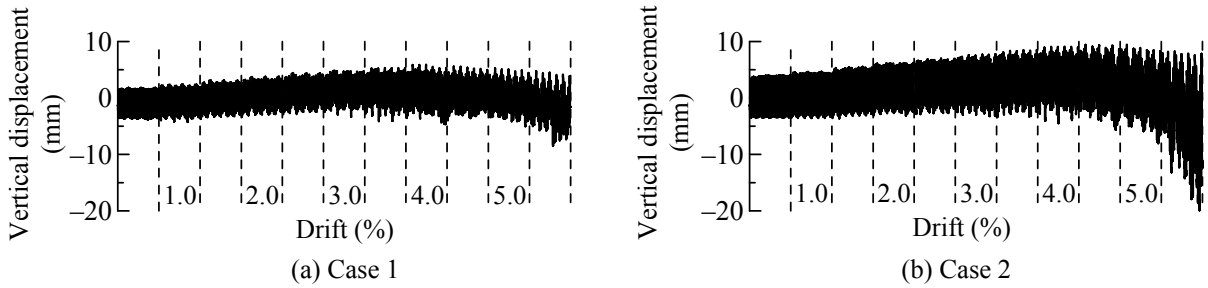


**Figure 11.** Vertical displacement at the column top

### 3.2. Lateral Force vs. Lateral Displacement Hysteresis

**Figure 7** shows the lateral force vs. lateral displacement hysteresis under Case 1-4. Hysteresis under Case 1 and 2 exhibited a unique behaviour due to the cyclic axial force variation including tension per cycle of lateral displacement. To investigate the mechanism of the hysteresis, lateral force vs. lateral displacement hysteresis and axial force vs. moment hysteresis at 3.5 % drift loading, respectively, are shown in **Figures 8** and **9**.

Under Case 1, restoring force was 146 kN under the peak compressive axial stress of  $3 \text{ N/mm}^2$  at point A. Restoring force became 102 kN under the peak tensile axial stress of  $1 \text{ N/mm}^2$  at point B, which was 70.2 % of the restoring force at point A. Restoring force increased again up to 163 kN due to the compressive axial stress of  $3 \text{ N/mm}^2$  at point C. The mechanism of variation in restoring forces from point D to F was similar with those from point A to C. Under Case 2, restoring force under the peak compressive and tensile axial force was 150 kN at point A and 81.8 kN at point B, respectively. Restoring force decreased as the peak tensile axial force increased. Flexural capacity varied linearly as axial force varied from  $2 \text{ N/mm}^2$  in tension to  $1 \text{ N/mm}^2$  in compression as shown in the envelop curve of moment-axial force relationship in **Figure 9 (b)**.

### 3.3 Accumulated Dissipated Energy

**Figure 10** shows the accumulated dissipated energy under Case 1-4. Accumulated dissipated energy at 3.5 % drift was 32.0 kN·m subjected to the constant compressive axial stress of  $3 \text{ N/mm}^2$  under Case 3. Compared with the accumulated dissipated energy under Case 3, accumulated dissipated energy was 25.3 kN·m under Case 1 (79.1 %), 23.6 kN·m under Case 2 (73.8 %) and 28.6 kN·m under Case 4 (89.4 %), respectively. The difference between Case 1 and 4 was the number of cycles of varying axial force per cycle of lateral displacement. It is shown that restoring force decreased extensively due to tension in the axial force variation in **Figure 8**, which resulted in a decrease of accumulated dissipated energy.

### 3.4 Vertical Displacement at the Column Top

**Figure 11** shows the vertical displacement at the column top. The vertical displacement at the column

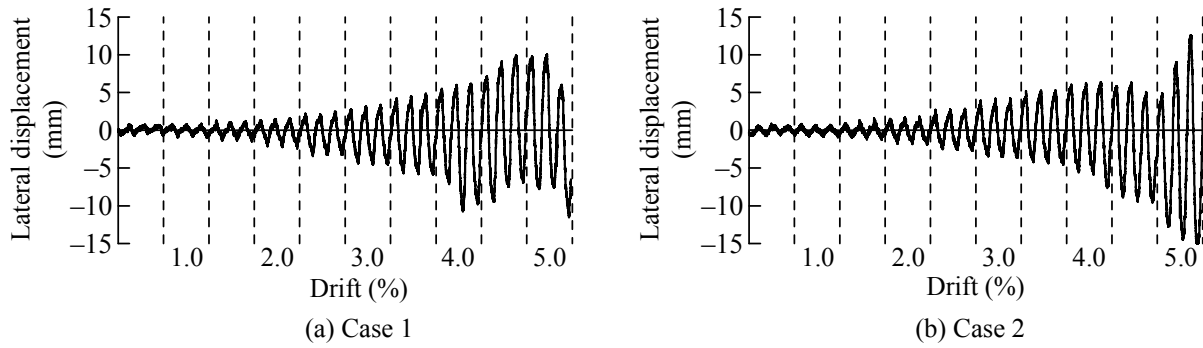


**Figure 12.** Lateral deformation in the plastic hinge region of the column

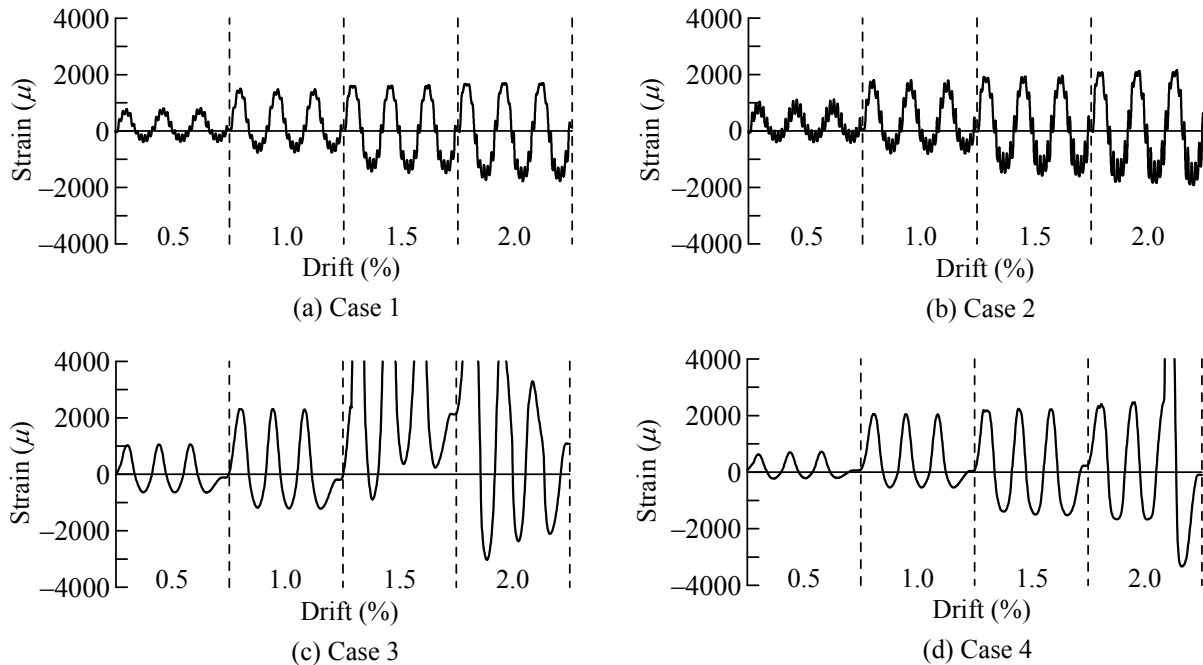


**Figure 13.** Strain of longitudinal bars along E face at 75 mm high from the column base

top was gradually caused upward due to the pull-off of longitudinal bars from the footing until 4.0 % drift loading, in which longitudinal bars started to buckle as mentioned before. On the other hand, the vertical displacement at the column top was caused downward due to the progress of damage of core concrete and buckling of longitudinal bars resulted from the reversed cyclic axial force variation.

The amplitude of the vertical displacement at 0.5 % and 5.5 % drift loading under Case 1 was 5 mm and 13 mm, respectively. Note that after 4.0 % drift loading, the amplitude extensively increased due to the damage progress of core concrete. The amplitude at 0.5 % and 5.5 % drift loading under Case 2 was 7 mm and 28 mm, respectively. This sharp increase in the vertical displacement at the column top shows the effect of the peak tensile axial force on the damage progress of core concrete due to the reversed cyclic axial force variation from tension to compression.

### 3.5 Lateral Deformation in the Plastic Hinge Region

**Figure 12** shows the lateral displacement at 400 mm high from the column base relative to the surface of footing. The lateral displacement at the plastic hinge significantly increased after the longitudinal bars buckled at 4.0 % drift loading under Case 1 as well as Case 2 due to the shear deformation resulted from the damage progress of core concrete and buckling of longitudinal bars. Shear deformation after the buckle of longitudinal bars increased as the peak tensile force in the axial force variation increased because the damage of core concrete increased.

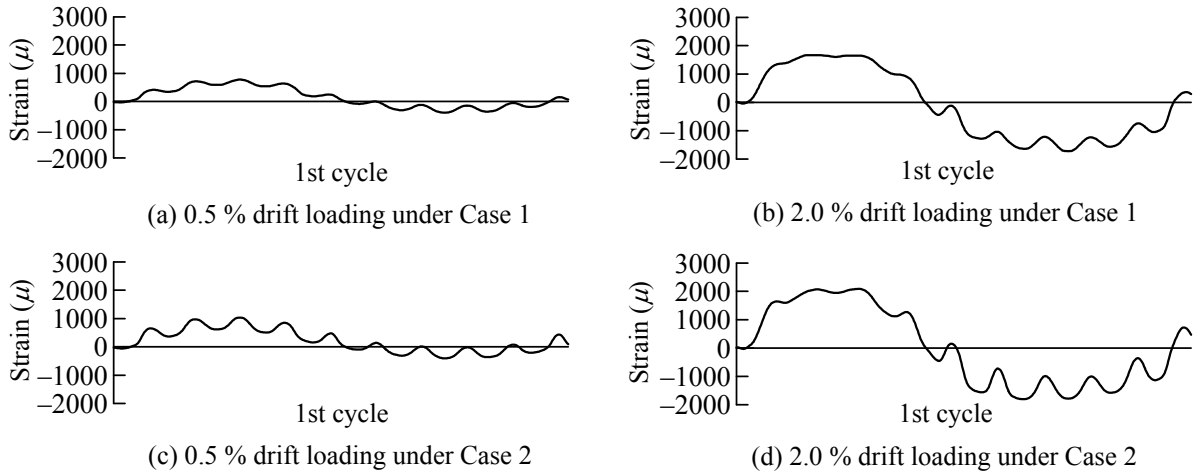


**Figure 14.** Strain variation due to the varying axial force

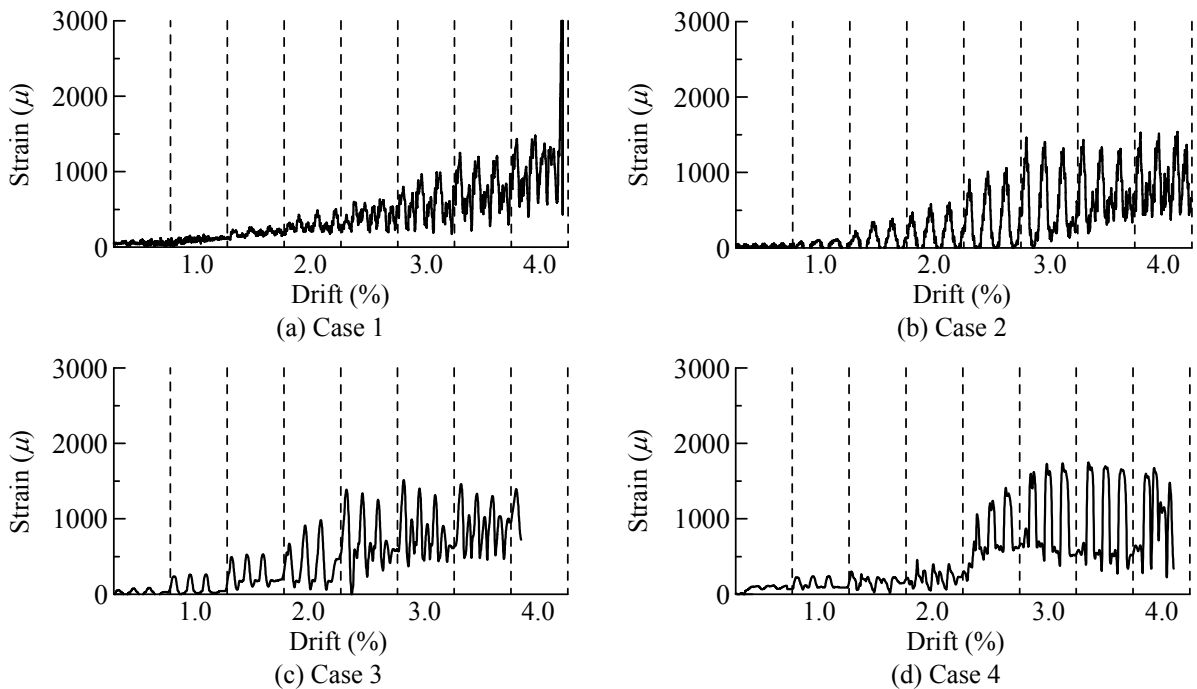


**Figure 15.** Strain of ties along S surface at 150 mm high from the column base

### 3.6 Strain of Longitudinal Bars and Ties

**Figure 13** shows the strain of longitudinal bars along E face at 75 mm high from the column base. Columns were subjected to the constant compressive axial stress of  $3 \text{ N/mm}^2$  under Case 3, and strain of longitudinal bars increased as drift increased. However, strain of longitudinal bars did not increase under Case 1, 2 and 4, in which tensile force was included in the axial force variation.

**Figure 14** shows an enlarged part of the 1st cycle of 0.5 % and 2.0 % drift loading under Case 1 and 2 in **Figure 13**. The strain variation consists of a long-period component and a short-period component. The long-period component was resulted from the cycle of lateral displacement, and the short-period component was resulted from the varying axial force. Strain variation due to the varying axial force was obvious both in tension and compression at 0.5 % drift loading. However, as shown in **Figure 13**, strain variation in tension due to the varying axial force was not clearly observed as drift increased. Regarding strain variation in compression due to the varying axial force, the amplitude of the strain variation of longitudinal bars due to the varying axial force increased as drift increased. For example, it was  $200 \mu$  and  $400 \mu$  at 0.5 % and 2.0 % drift loading under Case 1 as shown in **Figure 14** (a) and

(b), respectively, though the loading condition on the axial force variation was same at 0.5 % and 2.0 % drift loading. The same trend was also observed under Case 2. Amplitude of variation in the strain of longitudinal bars due to the varying axial force was  $400 \mu$  and  $800 \mu$  at 0.5 % and 2.0 % drift loading under Case 2 as shown in **Figure 14** (c) and (d), respectively. Strain variation due to the varying axial force was caused mainly at the compression side of the column as drift increased.

**Figure 15** shows the strain of ties along S face at 150 mm high from the column base. Tie bars yielded due to the buckling of longitudinal bars at 4.0 % drift loading as shown in **Figure 15** (a). Confining effect by ties is resulted from a passive mechanism due to Poisson's effect of core concrete, strain of tie bars became zero when the peak tensile axial force was imposed to the column.

#### 4. CONCLUSIONS

To clarify the effects of varying axial force including tension developed by the extreme vertical ground motions on the seismic performance of RC bridge columns, an experimental investigation was conducted based on cyclic loading experiments of RC columns under axial force variations. Based on the results presented herein, the following conclusions were deduced.

- 1) The damage of core concrete progressed extensively due to the reversed cyclic axial force variation from compression to tension after the longitudinal bars buckled, which resulted in the shear deformation in the plastic hinge region. Shear deformation after the buckle of longitudinal bars increased as the peak tensile force in the axial force variation increased because the damage of core concrete increased.
- 2) The damaged area of core concrete and the increase in the amplitude of the vertical displacement after the buckling of longitudinal bars due to the axial force variation became larger as the peak tensile force in the axial force variation increased.
- 3) Restoring force under tensile axial force decreased, which caused a decrease in the accumulated dissipated energy of the RC column. The decrease in the accumulated dissipated energy of the column became larger as the peak tensile axial force increased.

#### REFERENCES

- Button M. R., Cronin C. J., Mayes R. L. (2002). Effect of Vertical Motions on Seismic Response of Highway Bridges. *Journal of Structural Engineering*, ASCE. **128: 12**, 1551-1564.
- Japan Road Association (2002). Design Specifications of Highway Bridges - Part V Seismic Design. Maruzen, Tokyo, Japan.
- Kim, S. J., Holub, C. J. and Elnashai, A. S. (2011). Experimental Investigation of the Behavior of RC Bridge Piers subjected to Horizontal and Vertical Earthquake Motion. *Engineering Structures*. **33: 7**, 2221-2235.
- Kunnath, S. K., Erduran, E., Chai, Y. H. and Yashinsky, M. (2008). Effect of Near-Fault Vertical Ground Motions on Seismic Response of Highway Overcrossings. *Journal of Bridge Engineering*, ASCE. **13: 3**, 282-290.
- Papazoglou, A. J. and Elnashai, A. S. (1996). Analytical and Field Evidence of the Damaging Effect of Vertical Earthquake Ground Motion. *Earthquake Engineering and Structural Dynamics*. **25: 10**, 1109-1137.
- Sakai, J. and Kawashima, K. (2002). Effect of Varying Axial Loads including a Constant Tension on Seismic Performance of Reinforced Concrete Bridge Piers. *Journal of Structural Engineering*, JSCE. **48A**, 735-746.